Imaging of stem cell therapy in Acute Respiratory Distress Syndrome in sheep and its relationship with histopathology

Sirous Sadeghian Chaleshtori (s.sadeghian@ut.ac.ir)
Faculty of Veterinary Medicine
Mohammad Reza Mokhber Dezfouli
University of Tehran Faculty of Veterinary Medicine
Javad Abbasi
University of Tehran Faculty of Veterinary Medicine
Massoumeh Jabbari Fakhr
Qom University of Medical Sciences and Health Services School of Medicine
Alireza Vajhi
University of Tehran Faculty of Veterinary Medicine
Mohammad Reza Esmaeilnejad
University of Tehran Faculty of Veterinary Medicine
Saeed Farzad Mohajeri
University of Tehran Faculty of Veterinary Medicine

Research

Keywords: Imaging, stem cell therapy, ARDS, sheep.

Posted Date: November 13th, 2020

DOI: https://doi.org/10.21203/rs.3.rs-106506/v1

Abstract

Methods: 10 healthy sheep were separated as the control (PBS) and treatment(BM-MSCs). The BM-samples were aspirated in the treatment group and isolation and expansion of BM-MSCs were achieved. 24h after ARDS-induction by E.coli LPS (400 µg/kg), 5×10^7 BM-MSCs and 1 ml PBS were intrapulmonary infused in the treatment and control groups, respectively. The total lung volume and the Hounsfield unit by CT-scan and the cardiac parameters by echocardiography were calculated before of ARDS (time -24) and cells/PBS infusion time(time 0) and then for 6,12,24,48,72,168h after cells/PBS infusion. At the end, the sheep were sacrificed and the hearts and lungs were macroscopically and microscopically checked.

Results: The results showed the total lung volume and the Hounsfield unit increased at time 0, but BM-MSCs declined their amount, so that the changes were significant at 168h compared with time 0 and comparisons between the two-groups represented the significant difference at 72h and 168h. The cardiac parameters did not changes significantly in the two-groups at different times but the comparison between them demonstrated significant difference in LVPWs, IVSs,IVSd,%FS,$RVOT_{Vmax}$,LA(d1) and AO(d2) at 168 h, LVIDs,ESV and %EF at 72h and 168h and LVPWd at 72h. Also, the histopathology findings indicated decline of inflammatory reactions, edema, hemorrhage and hyperemia in the respiratory system and no observation of damage to the heart compared with the control-group.

Conclusions: The results determined BM-MSCs in ARDS decrease edema and inflammation of the lungs and increase the alveoli air volume and prevent damage to heart function.

Background

ARDS is one of the main and developing reason of respiratory failure. In very cases such as COVID-19, there is a complication by secondary severe ARDS (1). A particular characterize of ARDS is a decrease in aerated respiratory volume and diffuse alveolar damage (2). The clinical symptoms occur resulting from disruption of alveolar-capillary permeability and leakage of inflammatory cells, fluid and protein into spaces of interstitial and the alveoli (3). The current medical treatments in ARDS and some lung diseases are just supportive and cannot inhibit the disease progression (4, 5). Stem cell therapy is a new approach for ARDS treatment and the MSCs have a role in control of inflammation and tissue regeneration (6).

There are several techniques to evaluate the treatment process for ARDS and one of them is imaging. The diagnostic main landmark of ARDS is presence of bilateral infiltrates on the chest radiograph (bilateral radiographic opacities) (7, 8) and according to Berlin definition for the diagnosis of ARDS a conventional chest x-ray is obligate (9). But determining the exact cause and clinical complications of ARDS are difficult using radiology, only (10). The chest computed tomography (CT-scan) is a known and effective method to confirm the ARDS diagnosis and its role is critical to the disease process and the treatment further understanding and also, is a research technique in the experimental studies (8).The CT-scan is fast, painless, noninvasive, repeatable and accurate technique, which can calculate densities of lung and separated aerated from nonaerated lung zone (11, 12). The CT-scan uses to check abnormalities in

radiology and etc., and for diagnose the cause of inexplicable cough, dyspnea, lung inflammation and edema and the other signs. Nonetheless, there are some indications for CT-scan in ARDS that consisted of confirmation of diagnosis, calculation of recruitability, identification of a pulmonary or extrapulmonary cause, prediction of prognosis, and follow-up (8). Also recently CT-scan is using for diagnosis of the global pandemic COVID-19. COVID imaging pattern is consistent with ARDS and suggests that same physiological mechanism (1). Also according to the Berlin definition, the echocardiography use is recommended to evaluate function of cardiac at the time of suspected extrapulmonary causes and the absence risk factor of ARDS (7). Therefore, because imaging plays a key role in the diagnosis of ARDS and can provide disease progression and response to treatment, the present study was designed for evaluation of CT-scan and echocardiography in management and monitoring stem cells therapy in repair and regeneration ARDS in sheep and its comparison with evaluation of histopathology.

Materials And Methods

Study design

Sampling, isolation and characterization of BM-MSCs

Ten healthy male Shall sheep were randomly separated into the two groups of control (PBS, n = 5) and treatment (BM-MSCs, n = 5). All animal rights and ethics were performed according to the Animal Research Ethical Committee of University of Tehran (Tehran, Iran). The BM samples were aspirated in the treatment group from anaesthetized animal illiac crest with ketamine 10% 35 mg/kg (Alfasan-Holland), and xylazine 2% 5 mg/kg (Interchemie-Holland). Isolation and expansion of BM-MSCs were achieved by a protocol explained perviosly (13). For characterization, the BM-MSCs were tracked with antibodies of PE-conjugated versuse CD44, CD29 and CD31 (Abcam, Inc), CD45 (Biolegend, Inc) and were checked by flow cytometry (BD Bioscience, USA) and ability to differentiate BM-MSCs was evaluated via specific staining for osteogenic and adipogenic lineages.

Experimental Procedure

ARDS experimental model and BM-MSCs autologous transplantation in sheep were carry outed by a protocol explained perviosly (14). Briefly, all sheep in the two group were anesthetized and LPS at dose 400 µg/kg were intrapulmonary injected. Then, according to Berlin definition, ARDS was proved based on findings of radiography. 24 h after ARDS induction, 5×10^7 BM-MSCs and 1 ml PBS were intrapulmonary infused in the treatment and control groups, respectively. The sheep in the two group were imaged by CT-scan for lung evaluation and echocardiography before of ARDS (time − 24) and cells/PBS infusion time (time 0) and after for 6, 12, 24, 48, 72, 168 h after cells/PBS infusion.

Imaging

Radiography

The chest radiographic examination was done befor starting the study to check the lung and heart health and after to confirm ARDS. The sheep were exited from the study with radiographic evidences of disoreders of pulmonary and cardiac. For these purposes, two standard chest radiographs, ventro-dorsal and lateral, were done with equipment of digital X-ray Kodak carestream directview classic CR (Toshiba), and the factors of techniqal 70 Kv and 3.2 mA/s for every sheep.

Computerized Tomography Scan (CT-scan)

For examination of CT-scan, first, each sheep was anaesthetized with xylazine and ketamine and then, placed in sternal recumbency and head toward the gantry. After, the plain CT-scan was done with the equipment of Somatoma Spirit class II (Siemens), and the factors of technical 130 Kv, 75–95 mA, time of rotation: 1, thickness of slice: 1 mm and pitch: 1, from apical thoracic inlet until L2. All obtained images were renewed into windows of pulmonary and soft tissue. Then the total lung volume (intraalveolar space) and the Honsfield unit were calculated for each animal using the Pomona technique in volumetric software on the computer system of Leonardo. Margins of lung parenchymal were manually identified, and Hounsfield units mean were determined for each section and the pattern of 3D was viewed for more detail check of the lung parenchyma. The CT-scan assessment was done at times of -24 h (before ARDS inducing), 0 (cells/PBS infusion), 24, 48, 72 and 168 h after cells/PBS infusion.

Echocardiography

First, the sheep were placed standing with stretched forelimbs and then by a GE ultrasound unit Vivid 7 model (Norway) with a phased-array transducer of 4.4–10.0 MHz was done evaluation of echocardiographic included two-dimensional, M-mode and Pulsed-wave Doppler echocardiography in view of right parasternal trans-thoracic. Evaluation of trans-thoracic echocardiography was done for determine disorders of cardiologic, conventional hematological, physical and heart function with designate parameters of LVID, LVPWs, LVPWd, IVSs, IVSd, SV, FS, EF, ESV, EDV, RVOT $_{Vmax}$, RVOT $_{Vmean,}$ LVOT $_{Vmax}$, LVOT $_{Vmean}$, LA, AO and LA/AO. The echocardiography parameters were saved at times − 24 h (before ARDS inducing), 0 (cells/PBS infusion), 6, 12, 24, 48, 72 and 168 h after cells/PBS infusion.

Histopathology

At the end the study, 7 days after BM-MSC transplantation/PBS infusion, the sheep were killed and for inspection and sampling, the chest was rifted, and the heart and lung were ligatured and dissected and were macroscopically checked and abnormal symptoms such as hyperemia, bleeding, edema, etc. were documented. Then, the histopathological slides were prepared as has been perviosly explained (13). The heart and lung were immersed in formalin 10% and the sections were commonly provided and with method of H&E were stained and then, by Nikon Optical Microscope (E600 Eclipse, Japan) viewed. Finally, a digital camera (u eye 2250) with a software of microbial version 2 provided images from samples.

Statistical analysis

From the SPSS program and the tests of independent samples t-test and repeated measure at the level $p < 0.05$ were used for statistical analysis of data and obtained information were expressed as mean ± SD.

Results

Sheep BM-MSCs characterizations

The Flow cytometric findings displayed that BM-MSCs represented cell surface antigen of CD44, 89% and CD29, 91% but did not represent CD45 and CD31, antigens of hematopoietic cells and endothelial cells, respectively. Also, ability to differentiate BM-MSCs via specific staining showed the MSCs maintained their differentiating potential to osteoblasts and adipocytes. These findings proved sheep cultured cells were BM-MSCs, which were applied in this study.

Findings of radiography

The radiography findings demonstrated the lungs were completely normal before the injection of LPS (Fig. 1, A and C), but 24 h after LPS injection, abnormal lung radiographies as mixed pattern with predominance of alveolar pattern observed (Fig. 1, B and D). Most conflicts observed in the posterior and dorsal regions of the lung. The findings confirmed the acute lung disorder and ARDS model.

Findings of CT-scan and histopathology of lung

Reduce edema and inflammations of the lung with MSCs

Hounsfield units and the total lung volume (intraalveolar space) of the left and right lungs calculated on different parts of CT with the computer system of Leonardo. Margins of lung parenchymal identified, manually and Hounsfield units mean determined for each part and the pattern of 3D viewed for more detail check of the lung parenchyma (Fig. 2, I).

The results of CT-scan showed at day the inflammation (time 0), the Hounsfield unit mean and the total lung volume increased which was indicative the enhancement in the production of mucus, edema, and acute inflammation (Fig. 2, II, B). The stem cells transplantation caused decline of the Hounsfield unit and the lungs volume mean at different imaging times compared with time 0, indicating an increase in air volume in the lung alveoli and decrease of edema and inflammation (Fig. 2, II, C). These changes (both Hounsfield unit and total lung volume) were significant in one week after the transplantation ($p=0.028$ and $p=0.013$, respectively) and comparisons between the two groups represented the significant difference at 72 h ($p=0.012$ and $p=0.030$, respectively) and 168 h ($p=0.036$ and $p=0.011$, respectively) (Fig. 2, III). In the control group, the increase in Hounsfield unit and total lung volume continued due to edema and inflammation until the end of the study (Fig. 2, III).

Histopathology findings revealed, transplantation of BM-MSCs was capable to decline edema and inflammation of the lungs and repair damaged structures. The lungs macroscopic evaluation indicated edema, hyperemia, the presence of secretions in airways, hemorrhage and hepatization in the group of

control, but slight edema and hyperemia seen in the group of treatment. The lungs microscopic evaluation in the treatment group displayed, the severity of inflammatory reactions, edema, hemorrhage and hyperemia reduced compared with the control group (Fig. 3E-F). In addition, the lesions and severity of inflammation in trachea, bronchi, and bronchioles were much less than the control group. So that, in trachea, the mild edema of the submucosa region and less infiltration of the inflammatory cells and in bronchi and bronchioles, slight hypermia and low number of monoclonal inflammatory cells observed.

But, evaluation of histopathology in the control group demonstrated severe hyperemia and hemorrhage and purulent acute inflammation so that, the pulmonary blood vessels, particularly the pulmonary arterioles and the alveoli capillaries were dilated and accumulated from blood (Fig. 3A). In these capillaries, a large number of leukocytes were predominantly polymorphonuclear (neutrophils and band cells). Neutrophils adhered to the inner surface of the capillary walls and following the marginalization and sequestration, these observed in intraalveolar space (Fig. 3B). In some samples, there were foci of purulent pneumonia with bronchitis and bronchiolitis (Fig. 3C). In the pleura, inflammation and severe edema (Fig. 3D) and in trachea, sever hyperemia and the edema of the submucosa region and the infiltration of single-nucleated inflammatory cells as multifocal observed.

The results of CT-scan and histopathology of the lung determined after inflammation, BM-MSCs transplantation decreased of edema and inflammation and repaired damaged structures and increased air volume in the alveoli.

Findings of echocardiography and histopathology of heart

MSCs causes prevent the decreased function and damage to the heart

According to statistical studies, the cardiac parameters measured with echocardiography of M-mode (Tables 1) and Doppler (Tables 2) did not change significantly after inflammation in the groups of treatment (ARDS+BM-MSCs) and control (ARDS+PBS) at different times. But the statistical comparison between the two groups demonstrated difference of significant in LVPWs at 168 h ($p=0.042$), LVPWd at 72 h ($p=0.006$), LVIDs at 72 h ($p=0.018$) and 168 h ($p=0.047$), IVSs at 168 h ($p=0.045$), (IVSd) at 168 h ($p = 0.048$), ESV 72 h ($p=0.045$), and 168 h ($p=0.042$), %FS at 168 ($p=0.037$), %EF at 72 h ($p=0.044$) and 168 h ($p=0.030$), $RVOT_{Vmax}$ at 168 h ($p=0.047$), LA (d1) at 168 h ($p=0.019$) and AO (d2) at 168 h ($p=0.041$). The photographs and parameters amounts of M-mode and Doppler echocardiography are demonstrated in fig. 4 and tables 1 and 2.

Table 1: The sheep parameters of M-mode echocardiography (mean± SD) in the treatment group (ARDS+BM-MSCs) and the control group (ARDS+PBS) in the study period

Echocardiography parameters	Times / Group	-24	0	6	12	24	48	72	168
LVPWs (mm)	Treatment	1.25±0.09	1.15±0.15	0.91±0.11	0.93±0.09	1.01±0.09	1.06±0.26	1.12±0.12	#1.24±0.29
	Control	1.24±0.08	1.12±0.14	1.02±0.20	1.08±0.12	0.96±0.10	1.07±0.09	1.16±0.10	1.28±0.06
LVPWd (mm)	Treatment	1.08±0.09	0.95±0.19	0.79±0.08	0.73±0.09	0.68±0.08	0.69±0.07	#0.76±0.18	0.90±0.06
	Control	1.05±0.21	0.82±0.12	0.75±0.12	0.87±0.12	0.73±0.06	0.80±0.08	0.79±0.04	0.85±0.09
LVIDs (mm)	Treatment	1.96±0.75	1.99±0.54	2.04±0.40	2.08±0.39	2.15±0.39	2.18±0.29	2.04±0.25	#2.06±0.29
	Control	2.04±0.02	2.08±0.28	2.07±0.28	2.16±0.13	2.35±0.19	2.36±0.15	2.20±0.03	2.36±0.04
LVIDd (mm)	Treatment	3.18±1.02	#3.06±0.51	2.94±0.54	3.19±0.33	3.33±0.33	3.29±0.28	3.30±0.26	3.25±0.22
	Control	3.52±0.86	3.45±0.21	3.10±0.47	3.24±0.23	3.25±0.27	3.26±0.32	3.27±0.21	3.12±0.15
IVSs (mm)	Treatment	1.38±0.26	1.20±0.17	1.06±0.11	1.0±0.12	1.04±0.10	1.10±0.19	1.15±0.14	#1.2±0.16
	Control	1.24±0.74	1.0±0.20	0.92±0.13	1.0±0.14	0.92±0.21	0.98±0.09	1.01±0.20	1.05±0.05
IVSd (mm)	Treatment	0.86±0.17	0.86±0.08	0.84±0.13	0.78±0.15	0.76±0.08	0.80±0.05	0.81±0.07	#0.86±0.07
	Control	0.80±0.06	0.79±0.12	0.77±0.19	0.83±0.09	0.81±0.13	0.83±0.15	0.88±0.09	0.94±0.13
FS (%)	Treatment	35.56±5.80	36.49±7.27	30.46±4.46	34.93±7.71	35.81±6.36	33.69±4.76	38.20±3.27	37.39±6.36
	Control	33.40±6.93	35.70±4.92	36.32±4.92	32.87±7.09	28.69±8.49	28.33±5.88	34.02±4.09	30.10±3.48
EF (%)	Treatment	67.45±7.73	69.55±11.35	59.39±6.51	64.89±9.92	66.13±9.31	63.53±6.71	#69.58±4.32	#68.28±8.14
	Control	62.16±7.15	66.23±6.16	67.08±6.63	62.11±9.85	55.62±12.87	53.62±8.78	60.98±8.93	55.34±4.14
SV (ml)	Treatment	30.80±20.70	32.82±18.43	26.53±12.20	26.39±5.59	29.72±6.07	27.89±5.15	30.74±4.73	29.43±6.22
	Control	27.48±15.44	29.42±6.55	28.90±7.85	26.85±8.12	25.87±10.40	25.63±9.21	29.69±6.17	25.96±4.04
ESV (mm)	Treatment	14.78±8.04	18.68±5.22	14.26±6.61	14.92±6.79	16.01±7.57	16.36±5.44	#13.75±4.37	#13.66±4.31
	Control	13.37±3.81	14.87±3.68	14.29±4.42	15.62±2.43	19.07±3.30	19.50±2.66	16.29±1.38	19.16±1.52
EDV (mm)	Treatment	45.57±12.30	38.05±15.41	34.80±15.58	41.31±10.63	45.74±11.09	44.25±9.20	44.50±8.65	43.09±7.24
	Control	44.29±8.48	36.94±7.74	39.19±19.0	42.48±7.28	45.14±8.75	45.14±9.57	45.98±6.27	44.07±2.89

#: The significant changes compared to the control group at the same time ($p < 0.05$).

Table 2: The sheep parameters of Doppler echocardiography (mean± SD) in the treatment group (ARDS+BM-MSCs) and the control group (ARDS+PBS) in the study period

Echocardiography parameters	Times / Group	-24	0	6	12	24	48	72	168
RVOT Vmax (cm/s)	Treatment	0.75±0.05	0.77±0.07	0.77±0.02	0.77±0.01	0.75±0.15	0.75±0.18	0.76±0.06	#0.75±0.04
	Control	0.74±0.15	0.75±0.15	0.77±0.08	0.77±0.04	0.76±0.03	0.76±0.11	0.74±0.11	0.72±0.17
LVOT Vmax (cm/s)	Treatment	0.88±0.07	0.94±0.08	0.99±0.03	1.05±0.12	0.98±0.13	0.89±0.19	0.87±0.25	0.81±0.26
	Control	0.86±0.06	0.94±0.05	0.99±0.03	1.19±0.26	0.97±0.37	0.90±0.08	0.84±0.14	0.82±0.07
LVOT Vmean (cm/s)	Treatment	0.36±0.03	0.38±0.07	0.40±0.06	0.43±0.04	0.40±0.03	0.36±0.03	0.36±0.06	0.37±0.03
	Control	0.35±0.05	0.37±0.04	0.38±0.04	0.41±0.05	0.42±0.07	0.41±0.04	0.43±0.07	0.41±0.11
LA (d1) (mm)	Treatment	2.83±0.47	2.86±0.43	2.84±0.64	2.74±0.21	2.94±0.34	2.73±0.32	3.0±0.51	#2.95±0.80
	Control	2.77±0.55	2.79±0.53	2.61±0.40	2.71±0.65	2.74±0.35	2.77±0.38	3.04±0.39	2.61±0.16
AO (d2) (mm)	Treatment	2.25±0.25	2.37±0.21	2.35±0.19	2.11±0.24	2.21±0.17	2.26±0.05	2.40±0.15	#2.48±0.11
	Control	2.14±0.37	2.25±0.32	2.22±0.30	2.42±0.42	2.17±0.38	2.28±0.37	2.24±0.43	2.24±0.96
LA/AO	Treatment	80.27±8.05	78.35±8.86	84.68±13.89	77.23±11.49	75.88±10.23	83.64±8.89	81.07±8.54	88.43±18.52
	Control	83.40±14.05	81.37±5.82	85.46±4.68	84.94±20.44	79.29±9.06	82.65±9.26	72.22±12.11	75.84±10.87

#: The significant changes compared to the control group at the same time ($p < 0.05$).

Histopathology findings displayed, BM-MSCs transplantation was able to prevention of damage to the heart. In the heart microscopic check in the MSCs receiver group viewed much less damage than the

control group (Fig. 5C-D). While, in the PBS receiver group determined hyperemia, presence of polymorphonuclear leukocytes in the capillaries and neutrophils penetrate into the heart muscle and caused myocarditis (Fig. 5A) and cardiomyolysis (Fig. 5B). The results of echocardiography and histopathology of the heart showed after inflammation, BM-MSCs transplantation improved cardiac parameters and prevented damage to heart function, while in the control group there was the damage to heart function.

Discussion

ARDS is one of the developing reason of respiratory failure which is characterized by a decrease in aerated respiratory volume and diffuse alveolar damage (15). Also, the main complication in global pandemic COVID-19 is a secondary severe ARDS and the alveolar cells damage is the main reason of ARDS related to COVID-19 (1, 16). Stem cells have effects of positive in reducing acute pulmonary inflammation in the experimental models (13, 17, 18) and the imaging is a technique to evaluate the treatment process in ARDS. The CT-scan is an effective technique to evaluate the MSCs effects in lung and the echocardiography is recommended to assess function of cardiac.

The present study findings displayed the BM-MSCs caused decline of the Hounsfield unit and the lungs volume mean in CT-scan and improve the cardiac function and parameters in echocardiography and also, reduce edema and inflammation of the lungs and prevention of damage to the heart in histopathology. This study is the first imaging evaluation to the process of BM-MSCs effects in the treatment of ARDS experimental model in sheep in the world.

CT-scan has been used in the ARDS studies since the 1980s to represent heterogeneous pulmonary patterns (19). The advantage of this method is the close relationship between CT density and physical density of the lung. This feature shows quantitative information from the lung in different conditions based on the varying degrees of air present in the lung (11, 12). In CT-scans of ARDS, the alveolar volume of the lungs appears to be less than normal, due to a uniform pulmonary edema and alveolar collapse. Therefore, CT-scans carry outs a good estimate of pulmonary edema (20). In CT-scan surveys, increasing the Hounsfield unit and the total volume confirm the alveolar air replacement with mucus and cells of inflammatory and the occurrence of acute inflammation, which, is consistent with the results of this study on day zero. But, BM-MSCs therapy reduced the amount of these factors at different times of the study that indicates an increase in alveolar air volume and a decrease in lung inflammation.

Kobayashi et al., in ARDS patients demonstrated relationship of radiology results with histopathology results, so that increasing lung attenuation in images of radiography and alveolitis and thickening of alveolar septal in histopathology observed which, their results are match with relationship the CT-scan and histopathology results of the present study (21). The results of the our previous study on the rabbit ARDS model (13), which are consistent with the results of this study, showed that the Hounsfield unit increased, one day after the inflammation, which confirmed the increase in the production of mucus, edema and acute inflammation. Nevertheless, stem cells transplantation led to a decline in the Hounsfield

unit, which was significant at 48, 72, and 168 h, indicating an enhancement in the alveolar air. In addition, according to statistical studies, the mean volume of the lung increased after inflammation, which cell therapy resulted in a decrease in this process that was significant at 72 and 168 h (13).

Echocardiography is a procedure of clinical diagnosis and prognostic to evaluate the performance of the heart in the ARDS. We indicated, which lung inflammation leads to alterations in parameters of echocardiography and decreases function of heart, but in the autologous BM-MSCs recipient group there was no remarkable change in the echocardiography parameters and cardiac function. This suggests that stem cells transplantation was able to prevent the occurrence of these changes. The findings are consistent with our past survey on rabbits (13).

Histopathology evaluations in various studies have shown reduction of inflammation and edema after MSCs therapy in the pulmonary damage model. As the researchers have indicated decreasing edema, the thickness of the wall between the alveolar and bleeding in mice after treatment (17, 22, 23), reduce the inflammatory cells infiltration, edema and hemorrhage following the transplantation in rabbit (13) and decline in lung inflammation of sheep after the transplantation of human MSCs (24). But there were no significant changes in histopathological examination in the pig model (25). We also represented transplantation of BM-MSCs improved ARDS by decreasing changes of pathological. The histopathology results of the Zhou et al., study are matched with this study. They demonstrated BM-MSCs in rat gut contents aspiration-induced lung injury decrease the lung edema and inflammation (26).

In study, Rojas et al., evaluation of histopathology in the *E.coli* LPS-induced ARDS in sheep showed that the human BM-MSCs transplantation as intratracheal reduces the inflammation and edema severity (24).

In the other study, researchers have indicated MSCs transplantation as intravenous reduced lung inflammation and edema in rat 1 hour after intraperitoneal injection of oleic acid. So that, in histopathological examination, the number of neutrophils was declined (27).

UC-MSCs can control the inflammatory response in acute lung injury. Human UC-MSC transplantation 1 hour after LPS-induced acute pulmonary inflammation in mice, reduced pathological lesions and inflammatory response (28).

Conclusions

This research showed the BM-MSCs transplantation in the experimental model of ARDS in sheep repair damaged structures and prevent the damage progression to the functioning of the cardio-respiratory system by increasing the alveoli air volume and maintaining the contraction of the heart. These findings are very promising for the treatment of ARDS by bone marrow-mesenchymal stem cells and since the alveolar cells damage is the main reason of ARDS related to COVID-19, the BM-MSC offer an appropriate alternative for health care services in COVID-19.

List Of Abbreviations

ARDS: Acute Respiratory Distress Syndrome

COVID-19: Corona Virus Disease-19

BM-MSC: Bone Marrow Mesenchymal Stem/Stromal Cells

MSCs: Mesenchymal Stem/Stromal Cells

LPS: Lipopolysacaride

BM: Bone Marrow

PBS: Phosphate Buffer Solution

IM: Intramuscular

GMP: Good Mmanufacturing Practice

FBS: Fetal Bovine Serum

DMEM-HG: Dulbecco's Modified Eagle Medium-High Glucose

CT-Scan: Computerized Tomography Scan

LVID: Left Ventricular Internal Dimension

LVPWd: Left Ventricular Posterior Wall end diastole

LVPWs: Left Ventricular Posterior Wall end systole

IVSd: Interventricular Septum end diastole

IVSs: Interventricular Septum end systole

FS: Fractional Shortening

EF: Ejection Fraction

SV: Stroke Volume

EDV: End-Diastolic Volume

ESV: End-Systolic Volume

RVOT $_{Vmean}$: Right Ventricular Outflow Tract mean velocity

RVOT $_{Vmax}$: Right Ventricular Outflow Tract maximum velocity

LVOT $_{Vmean}$: Left Ventricular Outflow Tract mean velocity

LVOT $_{Vmax}$: Left Ventricular Outflow Tract maximum velocity

LA: Left Atrium diameter

AO: Aortic root diameter

H&E: Hematoxylin and eosin

UC-MSCs: Umbilical Cord-derived Mesanchymal Stem/Stromal Cells

ES-MSCs: Embryonic Stem cell-derived Mesanchymal Stem/Stromal Cells

Declarations

Ethics approval and consent to participate

All animal rights and ethics were performed according to the Animal Research Ethical Committee of University of Tehran (Tehran, Iran).

Consent for publication

Not applicable.

Availability of data and material

Authors want to share their data.

Competing interests

The authors declare that they have no competing interests.

Funding

No funding was received.

Authors' contributions

SSC; The study design, performed the cellular experiments, and prepared the initial, revision and finalization manuscript.

MRMD; The study design, commented on the data analysis and the revision and finalization of the manuscript.

JA; Performed clinical experiments, the laboratory studies and prepared the initial manuscript.

MJF; Performed the cellular experiments, the laboratory studies and prepared the initial manuscript.

AV: Performed, analysis and interpretation the data of imaging.

MRE: Performed the imaging experiments.

SFM: Performed the clinical experiments.

All authors read and approved the final manuscript.

References

1. Rogers CJ, Harman RJ, Bunnell BA, Schreiber MA, Xiang C, Wang FS, et al. Rationale for the clinical use of adipose-derived mesenchymal stem cells for COVID-19 patients. Journal of translational medicine. 2020;18(1):203.
2. Cardinal-Fernandez P, Lorente JA, Ballen-Barragan A, Matute-Bello G. Acute Respiratory Distress Syndrome and Diffuse Alveolar Damage. New Insights on a Complex Relationship. Annals of the American Thoracic Society. 2017;14(6):844-50.
3. Matthay MA, Zemans RL. The acute respiratory distress syndrome: pathogenesis and treatment. Annual review of pathology. 2011;6:147-63.
4. McIntyre LA, Moher D, Fergusson DA, Sullivan KJ, Mei SH, Lalu M, et al. Efficacy of Mesenchymal Stromal Cell Therapy for Acute Lung Injury in Preclinical Animal Models: A Systematic Review. PloS one. 2016;11(1):e0147170.
5. Mokhber Dezfouli MR, Sadeghian Chaleshtori S, Moradmand A, Basiri M, Baharvand H, Tahamtani Y. Hydrocortisone Promotes Differentiation of Mouse Embryonic Stem Cell-Derived Definitive Endoderm toward Lung Alveolar Epithelial Cells. Cell journal. 2019;20(4):469-76.
6. Sadeghian Chaleshtori S, Mokhber Dezfouli MR, Jabbari Fakhr M. Mesenchymal stem/stromal cells: the therapeutic effects in animal models of acute pulmonary diseases. Respiratory research. 2020;21(1):110.
7. Matthay MA, Zemans RL, Zimmerman GA, Arabi YM, Beitler JR, Mercat A, et al. Acute respiratory distress syndrome. Nature reviews Disease primers. 2019;5(1):18.
8. Sheard S, Rao P, Devaraj A. Imaging of acute respiratory distress syndrome. Respiratory care. 2012;57(4):607-12.
9. Ranieri Vm Fau - Rubenfeld GD, Rubenfeld Gd Fau - Thompson BT, Thompson Bt Fau - Ferguson ND, Ferguson Nd Fau - Caldwell E, Caldwell E Fau - Fan E, Fan E Fau - Camporota L, et al. Acute respiratory distress syndrome: the Berlin Definition. (1538-3598 (Electronic)).
10. Kobayashi H, Itoh T, Sasaki Y, Konishi J. Diagnostic imaging of idiopathic adult respiratory distress syndrome (ARDS)/diffuse alveolar damage (DAD) histopathological correlation with radiological imaging. Clinical Imaging. 1996;20(1):1-7.

11. Gattinoni L, Pesenti A, Avalli L, Rossi F, Bombino M. Pressure-volume curve of total respiratory system in acute respiratory failure. Computed tomographic scan study. The American review of respiratory disease. 1987;136(3):730-6.
12. Chiumello D, Mongodi S, Algieri I, Vergani GL, Orlando A, Via G, et al. Assessment of Lung Aeration and Recruitment by CT Scan and Ultrasound in Acute Respiratory Distress Syndrome Patients. Critical care medicine. 2018;46(11):1761-8.
13. Mokhber Dezfouli MR, Jabbari Fakhr M, Sadeghian Chaleshtori S, Dehghan MM, Vajhi A, Mokhtari R. Intrapulmonary autologous transplant of bone marrow-derived mesenchymal stromal cells improves lipopolysaccharide-induced acute respiratory distress syndrome in rabbit. Crit Care. 2018(1466-609X (Electronic)).
14. Abbasi J, Mokhber Dezfouli MR, Sadeghian Chaleshtori S, Dehghan MM, Vajhi A, Baharvand H, et al. Improvement of clinical signs in experimental model of Acute Respiratory Distress Syndrome (ARDS) in sheep following autograft of bone marrow-derived mesenchymal stem cells (BM-MSCs)2018. 17-26 p.
15. Cardinal-Fernández PA-O, Lorente JA, Ballén-Barragán A, Matute-Bello G. Acute Respiratory Distress Syndrome and Diffuse Alveolar Damage. New Insights on a Complex Relationship. (2325-6621 (Electronic)).
16. Li X, Ma XA-O. Acute respiratory failure in COVID-19: is it "typical" ARDS? (1466-609X (Electronic)).
17. Mei SHJ, McCarter SD, Deng Y, Parker CH, Liles WC, Stewart DJ. Prevention of LPS-Induced Acute Lung Injury in Mice by Mesenchymal Stem Cells Overexpressing Angiopoietin 1. PLoS Medicine. 2007;4(9):e269.
18. Rojas M, Parker RE, Thorn N, Corredor C, Iyer SS, Bueno M, et al. Infusion of freshly isolated autologous bone marrow derived mononuclear cells prevents endotoxin-induced lung injury in an ex-vivo perfused swine model. Stem cell research & therapy. 2013;4(2):26.
19. Chiumello D, Froio S, Bouhemad B, Camporota L, Coppola S. Clinical review: Lung imaging in acute respiratory distress syndrome patients–an update. Critical care. 2013;17(6):243.
20. Caironi P, Carlesso E, Gattinoni L. Radiological imaging in acute lung injury and acute respiratory distress syndrome. Seminars in respiratory and critical care medicine. 2006;27(4):404-15.
21. Kobayashi H, Itoh T, Sasaki Y, Konishi J. Diagnostic imaging of idiopathic adult respiratory distress syndrome (ARDS)/diffuse alveolar damage (DAD) histopathological correlation with radiological imaging. Clin Imaging. 1996;20(1):1-7.
22. Gupta N, Krasnodembskaya A Fau - Kapetanaki M, Kapetanaki M Fau - Mouded M, Mouded M Fau - Tan X, Tan X Fau - Serikov V, Serikov V Fau - Matthay MA, et al. Mesenchymal stem cells enhance survival and bacterial clearance in murine Escherichia coli pneumonia. Thorax. 2012(1468-3296 (Electronic)).
23. Li Y, Xu J, Shi W, Chen C, Shao Y, Zhu L, et al. Mesenchymal stromal cell treatment prevents H9N2 avian influenza virus-induced acute lung injury in mice. Stem Cell Research & Therapy. 2016;7:159.

24. Rojas M, Cárdenes N, Kocyildirim E, Tedrow JR, Cáceres E, Deans R, et al. Human adult bone marrow-derived stem cells decrease severity of lipopolysaccharide-induced acute respiratory distress syndrome in sheep. Stem cell research & therapy. 2014;5(2):42-.
25. Moodley Y, Sturm M, Shaw K, Shimbori C, Tan DB, Kolb M, et al. Human mesenchymal stem cells attenuate early damage in a ventilated pig model of acute lung injury. Stem Cell Research. 2016(1876-7753 (Electronic)).
26. Zhou J, Jiang L, Long X, Fu C, Wang X, Wu X, et al. Bone-marrow-derived mesenchymal stem cells inhibit gastric aspiration lung injury and inflammation in rats. Journal of cellular and molecular medicine. 2016;20(9):1706-17.
27. Xu YL, Liu Yl Fau - Wang Q, Wang Q Fau - Li G, Li G Fau - Lu X-D, Lu Xd Fau - Kong B, Kong B. Intravenous transplantation of mesenchymal stem cells attenuates oleic acid induced acute lung injury in rats. Chin Med J (Engl)Chin Med J (Engl). 2012(0366-6999 (Print)).
28. Zhu H, Xiong Y, Xia Y, Zhang R, Tian D, Wang T, et al. Therapeutic Effects of Human Umbilical Cord-Derived Mesenchymal Stem Cells in Acute Lung Injury Mice. Scientific Reports. 2017(2045-2322 (Electronic)).

Figures

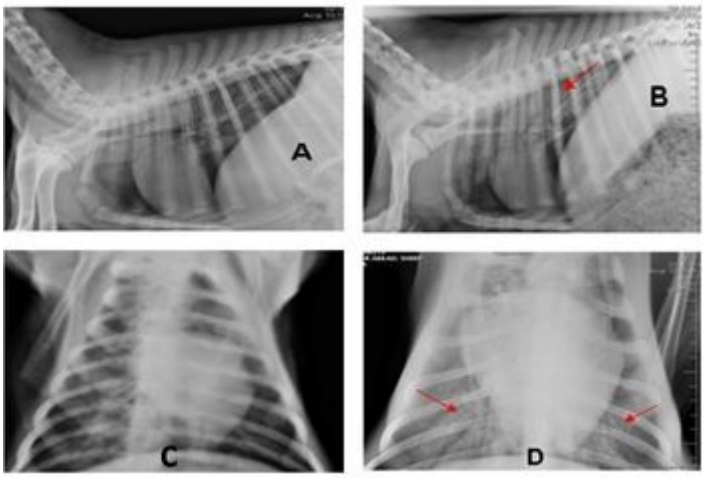

Figure 1

The sheep thorax radiography. Latteral view: (A) the normal lung before the LPS injection, (B) the inflammated lung 24 h after LPS injection (arrow). Ventrodorsal view: (C) the normal lung before the LPS injection, (D) the inflammated lung 24 h after LPS injection (arrows).

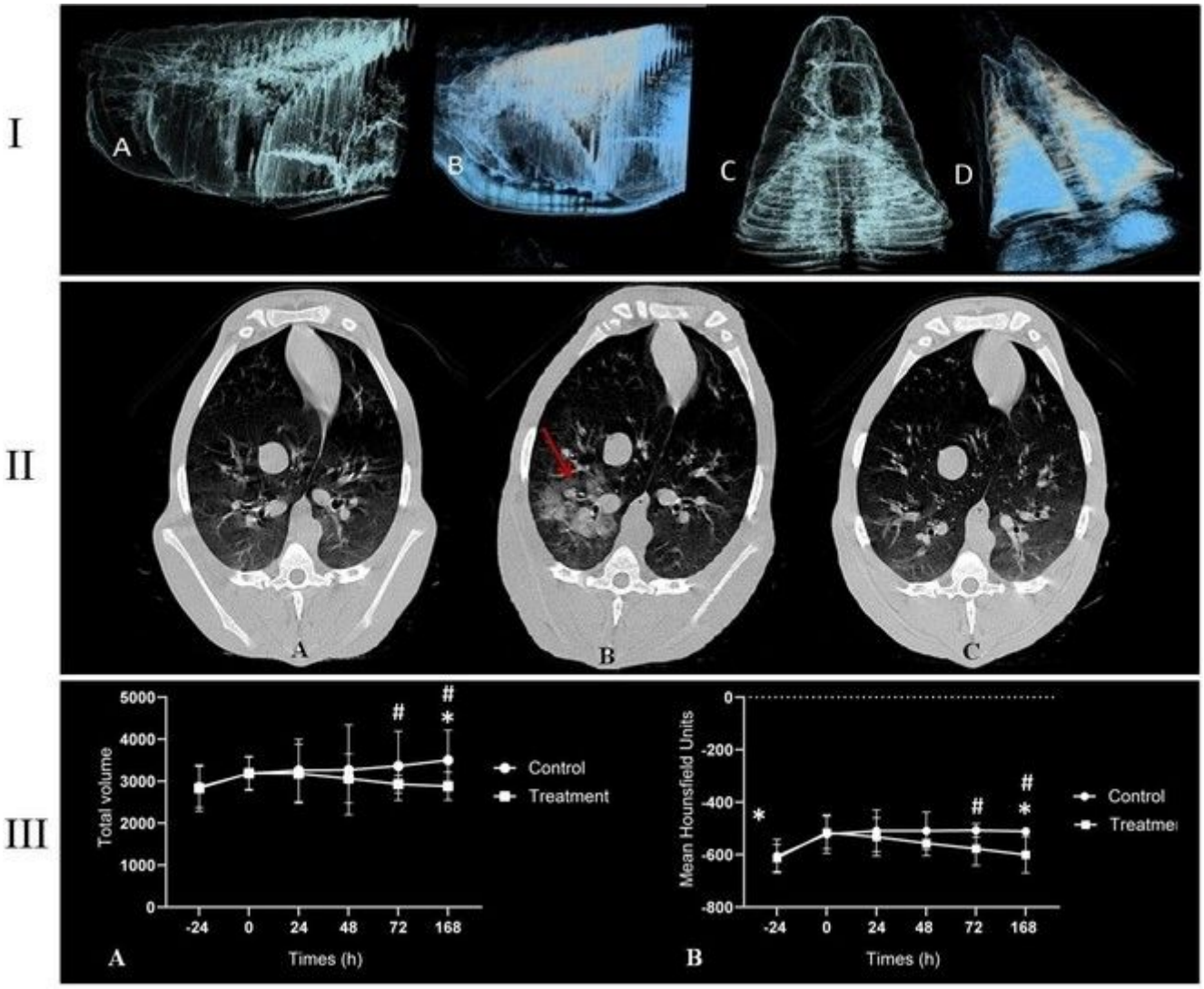

Figure 2

Sheep lung CT-scan analysis. I: 3D image of lung in pulmonary view. The treatment group (ARDS+BM-MSCs) (A and C). The control group (ARDS+PBS) (B and D). II: High-resolution the chest CT-scans (lung window) in the sheep. (A) Lung transverse section in healthy sheep, before ARDS (time -24). (B) Increased lung attenuation after ARDS (time 0) (arrow). (C) Decreased lung attenuation after BM-MSCs transplantation (time 168). III: The sheep lung CT-scan volumetry amount (the total lung volume and Hounsfield unit mean) (mean±SD) in the group of treatment and the group of control in the study period. (A) The total lung volume (intraalveolar space), (B) The Hounsfield unit mean. #: The significant changes compared to the control group at the same time ($p < 0.05$). *: The significant changes compared to zero time in the same group ($p < 0.05$).

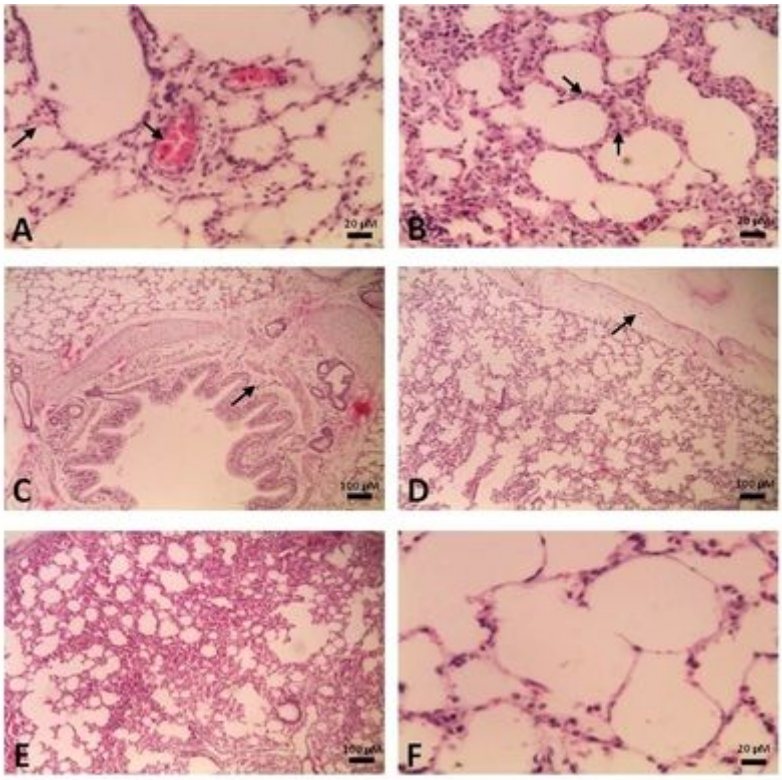

Figure 3

Histopathology of Sheep lung. The control group (ARDS+PBS), A: Severe hyperemia in the alveoli capillaries (arrows). B: Hyperemia and accumulation of polymorphonuclear cells in the alveoli wall, which is a sign of the onset of purulent pneumonia (arrows). C: Accumulation of inflammatory cells in the submucosa of the bronchus wall and the occurrence of bronchitis (arrows). D: Inflammation and severe edema of the pleura (arrows). The treatment group (ARDS+BM-MSCs), E-F: The microscopic examination displayed a decline in injury of the lung parenchyma and the alveoli.

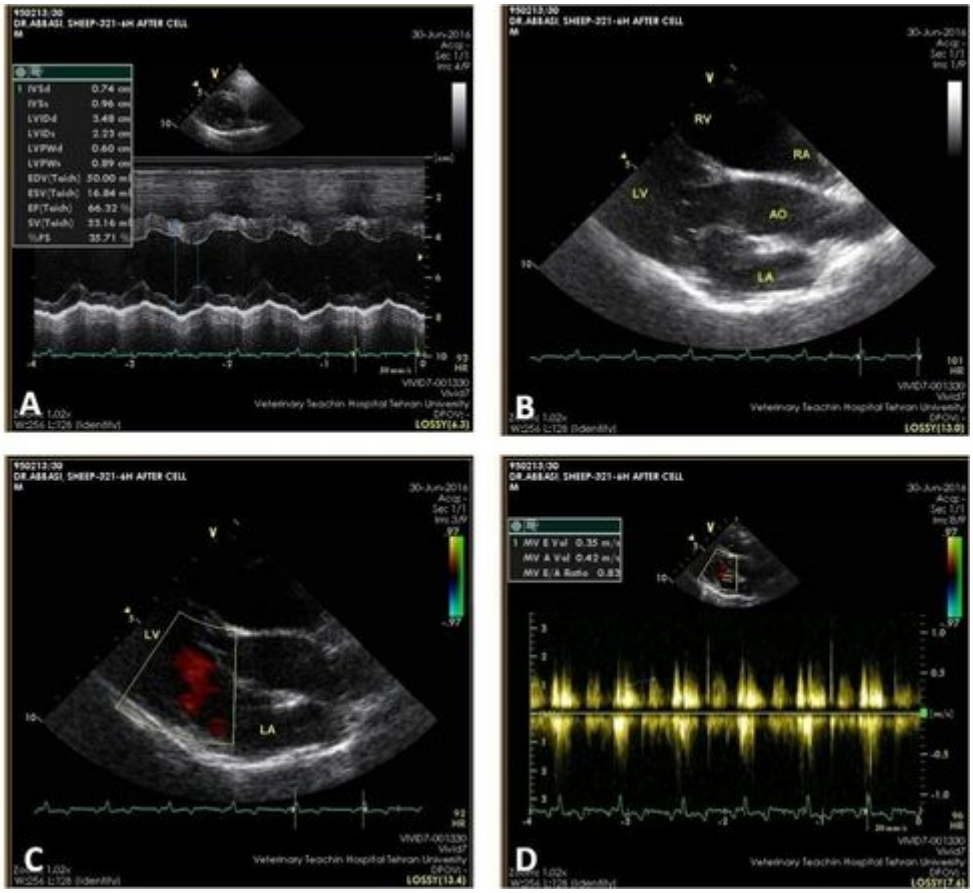

Figure 4

Sheep echocardiograms. (A) M-mode of the left ventricle. The interventricular septum (IVS), the left ventricular chamber, the left ventricular posterior wall (LVPW) and pericardium are visible. (B) The right parasternal long axis left ventricular outflow view: RA= right atrium, RV= right ventricle, LA= left atrium, LV= left ventricle and AO= aorta. (C) The Doppler echocardiography of the mitral valve. Flow from LA into LV on the right parasternal long axis left ventricular outflow view: LA= left atrium and LV= left ventricle. (D) Continuous wave doppler echocardiography of the mitral valve. Systolic and diastolic flows are positive whereas flow during contraction of atrium is negative.

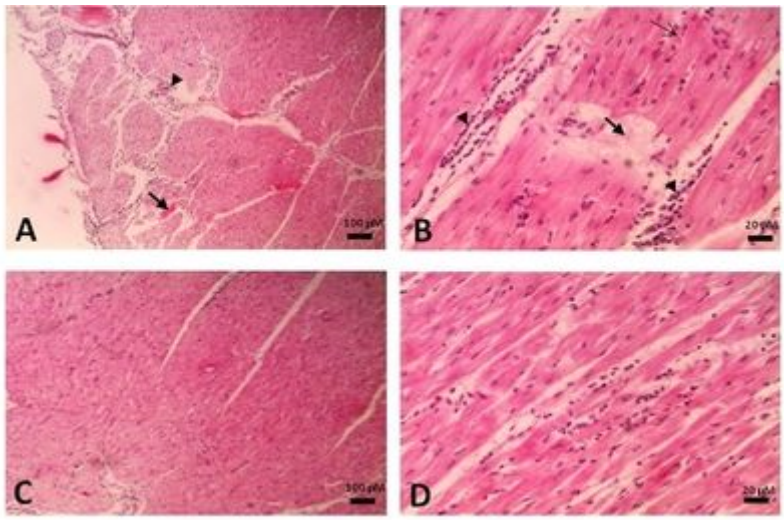

Figure 5

Histopathology of Sheep heart. The control group (ARDS+PBS), A: Hyperemia (arrows) and neutrophils accumulation (arrows heads) between the heart cells and occurrence of myocarditis. B: Hyperemia (thin arrow), neutrophils accumulation (arrows heads) and destruction of heart muscle cells (cardiomyolysis) (thick arrow). The treatment group (ARDS+BM-MSCs), C-D: The microscopic examination demonestrated much less damage than the control group.